Development 137, 3477-3487 (2010) doi:10.1242/dev.052761


# Atoh1a expression must be restricted by Notch signaling for effective morphogenesis of the posterior lateral line primordium in zebrafish

**Miho Matsuda and Ajay B. Chitnis***

## SUMMARY

The posterior lateral line primordium (pLLp) migrates caudally, depositing neuromasts to establish the posterior lateral line system in zebrafish. A Wnt-dependent FGF signaling center at the leading end of the pLLp initiates the formation of 'proneuromasts' by facilitating the reorganization of cells into epithelial rosettes and by initiating *atoh1a* expression. Expression of *atoh1a* gives proneuromast cells the potential to become sensory hair cells, and lateral inhibition mediated by Delta-Notch signaling restricts *atoh1a* expression to a central cell. We show that as *atoh1a* expression becomes established in the central cell, it drives expression of *fgf10* and of the Notch ligand *deltaD*, while it inhibits expression of *fgfr1*. As a source of Fgf10, the central cell activates the FGF pathway in neighboring cells, ensuring that they form stable epithelial rosettes. At the same time, DeltaD activates Notch in neighboring cells, inhibiting *atoh1a* expression and ensuring that they are specified as supporting cells. When Notch signaling fails, unregulated *atoh1a* expression reduces Fgfr1 expression, eventually resulting in attenuated FGF signaling, which prevents effective maturation of epithelial rosettes in the pLLp. In addition, *atoh1a* inhibits *e-cadherin* expression, which is likely to reduce cohesion and contribute to fragmentation of the pLLp. Together, our observations reveal a genetic regulatory network that explains why *atoh1a* expression must be restricted by Notch signaling for effective morphogenesis of the pLLp.

**KEY WORDS: *mind bomb*, Posterior lateral line, Neuromasts, Morphogenesis, Zebrafish, Cadherins, FGF signaling, Lateral inhibition**

## INTRODUCTION

The lateral line is a sensory system in fish and amphibians that is designed to sense directional water movements (reviewed by Ghysen et al., 2007). It consists of neuromasts, which contain sensory hair cells and surrounding supporting cells. The posterior lateral line primordium (pLLp) migrates under the skin and periodically deposits neuromasts to establish the primary pLL system in zebrafish (see Movie 1 in the supplementary material). The pLL presents an extraordinary system with which to study how a sensory system assembles itself. It is a relatively simple system, the morphogenesis of which is easy to monitor in live embryos. Furthermore, the ability to manipulate and monitor the function of individual signaling pathways in zebrafish embryos has led to a framework for understanding how interactions between Wnt, FGF, Notch and chemokine signaling pathways have a crucial role in directing the self-organization of this system (reviewed by Ma and Raible, 2009).

The migrating pLLp contains three to four 'proneuromasts' at various stages of maturation. As each proneuromast matures within the migrating pLLp, it forms a center-oriented epithelial rosette with a central *atoh1a*-expressing cell (Lecaudey et al., 2008; Nechiporuk and Raible, 2008). Eventually, a neuromast is deposited from the trailing end of the migrating primordium. Expression of *atoh1a* gives central cells the potential to become sensory hair cells, while surrounding cells are specified as supporting cells (reviewed by Ma and Raible, 2009). Supporting cells can proliferate and serve as progenitors that give rise to additional hair cells during growth and regeneration (Ma et al., 2008).

The formation of proneuromasts at the leading end of the migrating pLLp is initiated by two mutually antagonistic signaling centers: a Wnt signaling center in a leading domain and an FGF signaling center in an adjacent trailing domain (reviewed by Ma and Raible, 2009; Aman and Piotrowski, 2008). Establishment of the FGF signaling center is initiated by FGF ligand produced at the leading end in response to Wnt pathway activation. However, Wnt activation also drives expression of an FGFR antagonist, *sef* (*il17rd* – Zebrafish Information Network), which prevents local activation of the FGF signaling pathway. Meanwhile, activation of the FGF signaling pathway in the adjacent domain drives the expression of a diffusible Wnt antagonist, Dkk1. This prevents activation of the Wnt pathway from spreading towards the trailing end of the pLLp and establishes coupled, yet mutually inhibitory, Wnt-FGF systems at the leading end of the pLLp.

Once activated, FGF signaling has two crucial functions: it initiates the formation of center-oriented epithelial rosettes and the expression of the bHLH transcription factor Atoh1a (Lecaudey et al., 2008; Nechiporuk and Raible, 2008). Atoh1a drives expression of the Notch ligand Delta, which activates its receptor, Notch, in adjacent cells, which in turn inhibits *atoh1a* expression in these cells. In this manner, 'lateral inhibition' ensures that *atoh1a* expression and hair cell fate are restricted to a central cell, while inhibition of *atoh1a* in surrounding cells ensures that they are specified as supporting cells. Failure of Notch signaling in this context allows an expansion of *atoh1a*-expressing cells at the cost of supporting cells (Itoh and Chitnis, 2001).

Laboratory of Molecular Genetics, Section on Neural Developmental Dynamics, Eunice Kennedy Shriver National Institute of Child Health and Human Development, National Institutes of Health, Bethesda, MD 20892, USA.

*Author for correspondence (chitnisa@mail.nih.gov)

**Accepted 20 August 2010**

Previous studies have shown that inhibition of Notch signaling with DAPT (Geling et al., 2002), which prevents γ-secretase-dependent cleavage of Notch, increases the number of *atoh1a*-expressing cells but does not interfere with the morphogenesis or deposition of neuromasts (Lecaudey et al., 2008; Nechiporuk and Raible, 2008). In addition, inhibition of *atoh1a* function with morpholinos inhibits hair cell development without affecting rosette formation or neuromast deposition (Lecaudey et al., 2008; Nechiporuk and Raible, 2008). These observations have suggested that neuromast morphogenesis is independent of *atoh1a*- and Notch-dependent determination of hair cell fate (Lecaudey et al., 2008; Nechiporuk and Raible, 2008).

Mind bomb 1 (Mib1; Mind bomb – Zebrafish Information Network) is a RING E3 ubiquitin ligase that ubiquitylates Notch ligands such as Delta. Ubiquitylation serves as a signal for endocytosis of Delta and is an essential step for effective activation of Notch in a neighboring cell (reviewed by D'Souza et al., 2008; Itoh et al., 2003). *mib1* mutants have a broad and severe loss of Notch signaling and have an excess of *atoh1a*-expressing cells (Itoh and Chitnis, 2001). In this study, we show that Notch signaling has a previously unappreciated role in determining morphogenesis of the pLLp. By comparing *mib1* mutants with embryos in which Notch signaling has been inhibited via other manipulations, we show that loss of Notch signaling clearly contributes to the aberrant morphogenesis of the pLLp in *mib1* mutants. Our investigation of the mechanism by which Notch influences pLLp morphogenesis has revealed a role for Notch-restricted *atoh1* expression in determining the pattern of FGF signaling in maturing proneuromasts. It shows how unregulated *atoh1a* expression has the potential to influence rosette formation, migration and the cohesive properties of cells in the pLLp.

## MATERIALS AND METHODS

### Fish maintenance and mutant strains

Zebrafish were maintained under standard conditions. The embryos were staged according to Kimmel et al. (Kimmel et al., 1995). The *mind bomb*, *mib*$^{ta52b}$, *mib*$^{m132}$, *mib*$^{m178}$ (Itoh et al., 2003; Jiang et al., 1996), *notch1a*, *deadly seven*, *des*$^{b420}$ (Gray et al., 2001) and *tg[cldnb:lynGFP]* (Hass et al., 2006) mutant and transgenic strains were described previously. Treatment with 100 μM DAPT (Calbiochem) was started at 20 hpf. SU5402 (Calbiochem) was used at 20 μM.

### Morpholino injections

All morpholino injections (1.5 ng each) were performed with co-injection of *p53*-MO (Robu et al., 2007). MOs were purchased from Gene Tools. Morpholinos used in this study were (5′ to 3′):

*notch1a*-MO, GAAACGGTTCATAACTCCGCCTCGG (Yeo et al., 2007);

*notch3*-MO, ATATCCAAAGGCTGTAATTCCCCAT (Yeo et al., 2007);

*atoh1a*-MO, TCTCTTGTATCCGTGCTCATTCCAT (Millimaki et al., 2007); and

*atoh1b*-MO, TCATTGCTTGTGTAGAAATGCATAT (Millimaki et al., 2007).

### Whole-mount in situ hybridization

Double in situ hybridization was performed as described previously (Jowett, 2001). RNA probes were synthesized using a DIG or FITC labeling kit (Roche). BM Purple (Roche) or BCIP/NBT substrate (Vector Laboratories) was used for single-labeled embryos. For double-labeled embryos, Fast-Red substrate (Roche) was used as the second chromogen after a 20-minute treatment with 0.1 M glycine pH 2.2. In situ hybridization results were imaged with a CCD camera mounted on a Zeiss Axioplan2 microscope.

### Immunohistochemistry

Immunohistochemistry was performed as described previously (Matsuda and Chitnis, 2009). Antibodies were: mouse anti-zebrafish DeltaD (zdD2, Abcam; dilution 1:400), mouse anti-ZO1 (Zymed; 1:500) and rabbit anti-Cldnb (kindly provided by Dr J. Hudspeth, Rockefeller University, NY, USA) (Lopez-Schier et al., 2004). Images were captured with a confocal microscope (LSM 510META, Carl Zeiss).

### Live imaging of lateral line morphogenesis

Live cell imaging was performed as described previously (Kamei and Weinstein, 2005). Images were taken with the confocal microscope every 5 minutes. Images taken at several *z*-planes were projected into single image using Zeiss Image software. Movies were generated by QuickTime Pro software.

## RESULTS

### Neuromast deposition and pLLp migration are aberrant when Notch signaling is inhibited

We used *tg[cldnb:lynGFP]* transgenic fish (Haas and Gilmour, 2006), which express membrane-tethered GFP in the pLL system to examine pLLp migration and morphogenesis,. Examination of deposited cell clusters in fixed embryos at 48 hours post fertilization (hpf) showed that in wild-type embryos, five proneuromasts (L1 to L5) were deposited in a periodic pattern over the trunk, whereas the last three neuromasts (L6 to L8) were located at the tip of the tail where the pLLp normally stops migrating (Fig. 1A,E). In *mib1* mutants, the distribution of deposited cell clusters was erratic and closely spaced after deposition of the second neuromast (Fig. 1B,F). Ultimately, pLLp migration stalled about half way to the tip of the tail (Fig. 1B,F). Deposited clusters were of variable size and sometimes two small, adjacent, partially fused rosettes were seen instead of a single, well-formed epithelial rosette (Fig. 1C,D). Although no problems in initiation of rosette formation were seen at the early stage of pLLp migration (data not shown), by 32 hpf there was a delay in the central accumulation of Claudin b (Cldnb) and a failure to recruit ZO1 (Tjp1 – Zebrafish Information Network) to central junctional complexes in *mib1*$^{m132}$ mutants (Fig. 1J,K), suggesting that *mib1* mutants eventually have defects in both the formation and maintenance of the epithelial rosettes.

To determine whether loss of Notch signaling contributes to aberrant morphogenesis, *mib1* mutants were compared with embryos in which Notch signaling was inhibited via other manipulations, including DAPT treatment and injection of morpholinos targeting Notch homologs. Three Notch receptors, *notch1a*, *notch1b* and *notch3*, are expressed in the migrating pLLp (see Fig. S1 in the supplementary material). As morpholinos to *notch1b* caused cell death, only morpholinos for *notch1a* and *notch3* were used to knock down Notch function. To reduce minor side effects resulting from simultaneous injection of two morpholinos, the *notch3* morpholino was injected into *notch1a* loss-of-function mutants (*deadly seven*, *des*$^{b420}$) (Gray et al., 2001).

Although DAPT treatment or knockdown of *notch1a* and *notch3* function (N1a/N3MO) partially inhibited Notch signaling (Lecaudey et al., 2008; Nechiporuk and Raible, 2008) (data not shown), it did not reduce expression of *her4* (see Fig. S2C,D in the supplementary material), a Notch target gene (Takke et al., 1999), the expression of which is lost in the *mib1* pLLp (see Fig. S2B in the supplementary material). By contrast, exposing N1a/N3MO embryos to DAPT (N1a/N3MO/DAPT) eliminated *her4* expression (see Fig. S2E in the supplementary material), suggesting that this combinatorial manipulation reduces Notch signaling in a manner that is more comparable to that in *mib1* mutants. Whereas pLLp morphogenesis was not significantly affected when embryos were

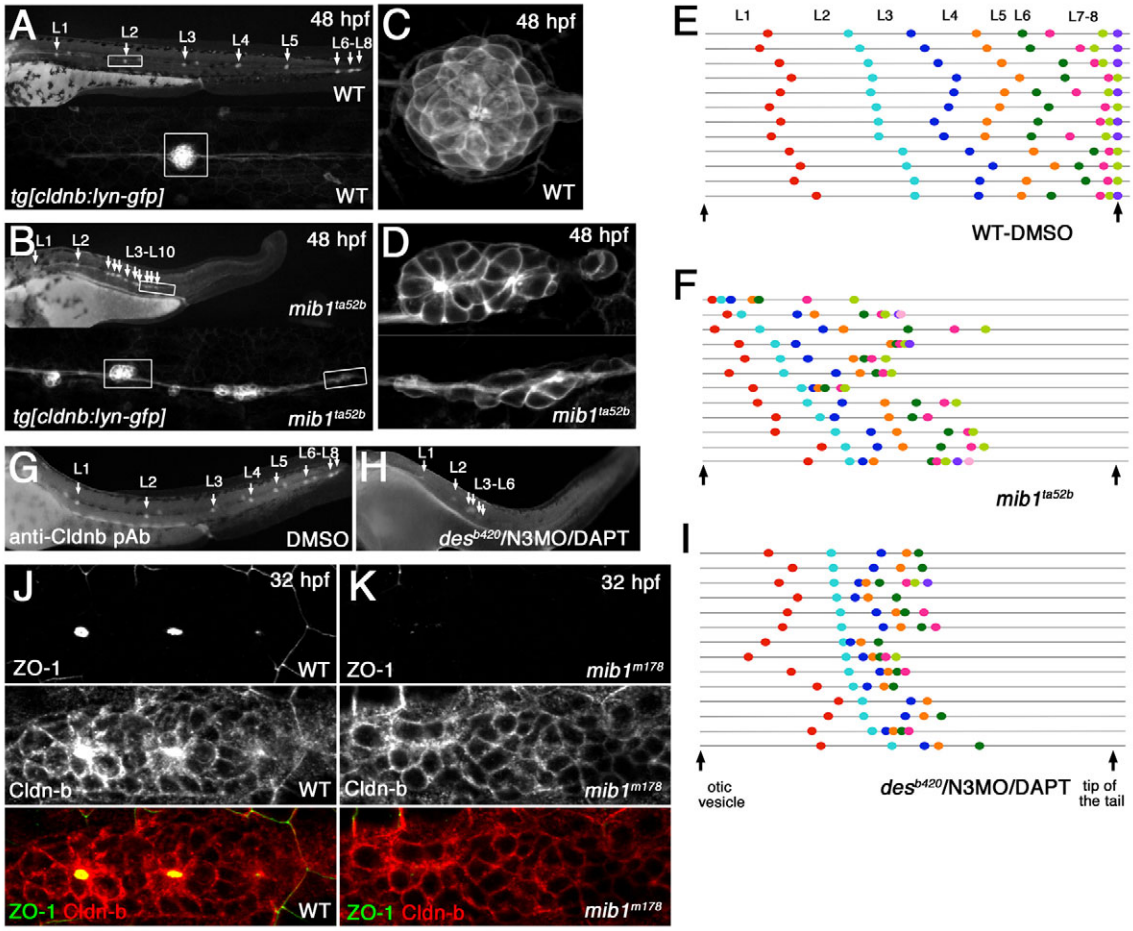


**Fig. 1. Loss of Notch signaling causes aberrant neuromast deposition and posterior lateral line primordium (pLLp) migration.** (**A-D**) The distribution and morphology of deposited neuromasts/cell clusters (L1 to L10) in (A,C) wild-type (WT) and (B,D) *mib1*$^{ta52b}$ *tg[cldnb:lynGFP]* zebrafish embryos at 48 hpf. (C,D) Epithelial rosettes are disorganized in *mib1*$^{ta52b}$ mutants. (**E**,**F**,**I**) The pattern of neuromast/cell cluster deposition at 48 hpf in individual wild-type (E), *mib1*$^{ta52b}$ (F) and *des*$^{b420}$/N3MO/DAPT (I) embryos. Colored dots show the position of each deposited neuromast/cell cluster relative to the otic vesicle and tail tip (vertical arrows). Individual embryos are represented on separate lines in an order determined by the relative position of L2. (**G**,**H**) The distribution of deposited neuromasts/cell clusters in DMSO-treated (G) and *des*$^{b420}$/N3MO/DAPT (H) embryos at 48 hpf. (**J**,**K**) There is no central accumulation of ZO1 and Cldnb accumulation is delayed in *mib1*$^{m178}$ neuromasts (K) when compared with the wild type (J) at 32 hpf.

only treated with DAPT or had Notch1a and Notch3 function reduced (data not shown), phenotypes similar to those seen in *mib1* mutants emerged when these manipulations were combined (Fig. 1G-I). These observations suggest that problems with pLLp morphogenesis can emerge when inhibition of Notch signaling is severe enough to eliminate *her4* expression.

Time-lapse imaging starting at 28 hpf showed that the erratic distribution of cell clusters deposited relatively early during pLLp migration in *mib1* embryos was in part due to poor cohesion of cells in depositing proneuromasts. Cells would often dissociate from a trailing proneuromast and then try to reassociate to form cell clusters with previously deposited cells (see Fig. S4B,E and Movie 2 in the supplementary material). This early defect in cell cohesion was not observed in N1a/N3MO/DAPT embryos (data not shown). However, time-lapse starting relatively late, at 32 hpf, showed that in both *mib1*$^{ta52b}$ and N1a/N3MO/DAPT embryos, ~3-5 hours after deposition of the second neuromast (L2), the migrating pLLp undergoes sudden fragmentation (Fig. 2B,C; see Movies 3, 4 in the supplementary material). This fragmentation accounts for the erratic distribution of cell clusters deposited relatively late during the migration. Following this fragmentation, a small fragment of the pLLp (Fig. 2B,C, bracket) continued to migrate as a much reduced collection of cells, until it too stopped migrating, suggesting that pLLp fragmentation contributes to the eventual failure of migration.

## Notch signaling regulates the expression of FGF signaling components

In *mib1* mutants, *atoh1a* expression is not effectively restricted to a central cell in maturing proneuromasts. Instead, its expression progressively expands to large cell clusters (termed 1° expansion) and then eventually to most of the cells within the migrating pLLp (termed 2° expansion) (Fig. 3A; see Fig. S5 in the supplementary material).

Expression of *fgf10* overlaps with *atoh1a* in maturing proneuromasts at the trailing end of the pLLp, where expression is typically restricted to a central cell in the wild-type pLLp (see Fig. S6A,B in the supplementary material). Consistent with their correlated expression, *mib1* mutants showed similar 1° and 2° expansion of *fgf10* expression (Fig. 3B; see Fig. S5 in the

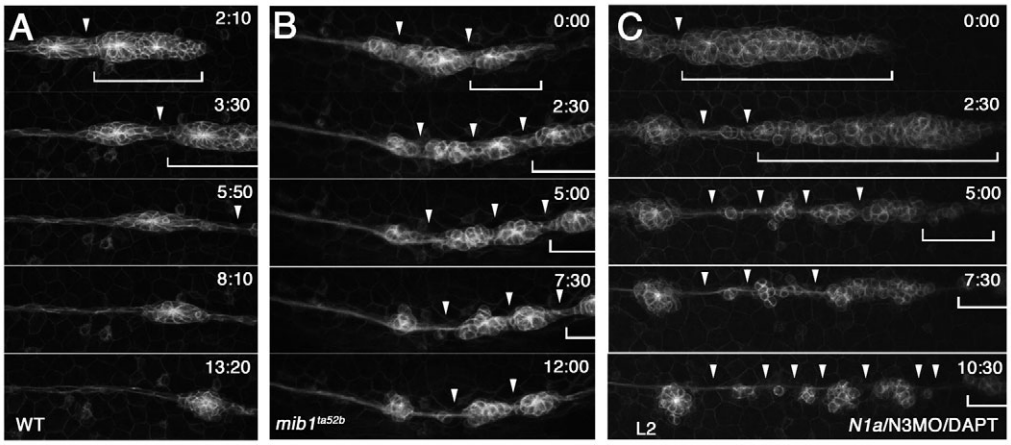


**Fig. 2. The pLLp eventually undergoes fragmentation when Notch signaling is lost.** Images from time-lapse (started at ~32 hpf) of (**A**) wild-type, (**B**) *mib1*$^{ta52b}$ and (**C**) N1/N3MO/DAPT *tg[cldnb:lynGFP]* zebrafish embryos. (A) In wild type, the pLLp migrates as a cohesive structure (bracket); a single break (arrowhead) allows deposition of a neuromast. See Movie 1 in the supplementary material. (B,C) The pLLp fragments as ectopic breaks develop (arrowheads), and proneuromasts are prematurely deposited in both *mib1*$^{ta52b}$ and N1/N3MO/DAPT embryos. A small portion of the remaining pLLp (bracket) continues to migrate. See Movies 3 and 4 in the supplementary material.

supplementary material). Furthermore, correlated expansion of *atoh1a* and *fgf10* was seen in *des*$^{b420}$/N3MO/DAPT embryos (see Fig. S7A-D in the supplementary material), confirming that expansion of both *atoh1a* and *fgf10* can result from loss of Notch signaling. Their correlated expression is consistent with *atoh1a* being responsible for driving *fgf10* expression in maturing neuromasts. Knocking down *atoh1a* and *atoh1b* function with morpholinos reduced *fgf10* expression at the trailing end of the pLLp (see Fig. S6C,D in the supplementary material), confirming that, as shown previously (Nechiporuk and Raible, 2008), *atoh1* determines *fgf10* expression in maturing proneuromasts.

## Expansion of *atoh1a* is accompanied by a complementary loss of *fgfr1* and FGF signaling

Although there is some overlap in their expression, *fgf10* and *fgfr1* are typically expressed in complementary patterns in the pLLp. As *fgf10* expression becomes restricted to a central cell in the maturing neuromasts, *fgfr1* is expressed in surrounding cells and reduced in the central cell (Lecaudey et al., 2008). This complementary relationship becomes more obvious in *mib1*$^{ta52b}$ (Fig. 3B,C) and *des*$^{b420}$/N3MO/DAPT embryos (see Fig. S7C-F in the supplementary material), in which expansion of central *fgf10*-expressing cells in maturing neuromasts is accompanied by a reduction of *fgfr1*-expressing cells. Initially, *fgfr1* expression was reduced in small clusters of cells (1° reduction). Eventually, it was broadly reduced in the pLLp and *fgfr1* expression was restricted to a few cells at its edges (2° reduction) (Fig. 3C; see Fig. S5 in the supplementary material).

Progressive reduction in *fgfr1* expression was accompanied by a reduction in expression of the FGF target gene *pea3* (Lecaudey et al., 2008; Nechiporuk and Raible, 2008) in *mib1*$^{ta52b}$ (Fig. 3D; see Fig. S5 in the supplementary material) and *des*$^{b420}$/N3MO/DAPT (see Fig. S7H in the supplementary material) embryos. This suggests that progressive expansion of *atoh1a* is associated with

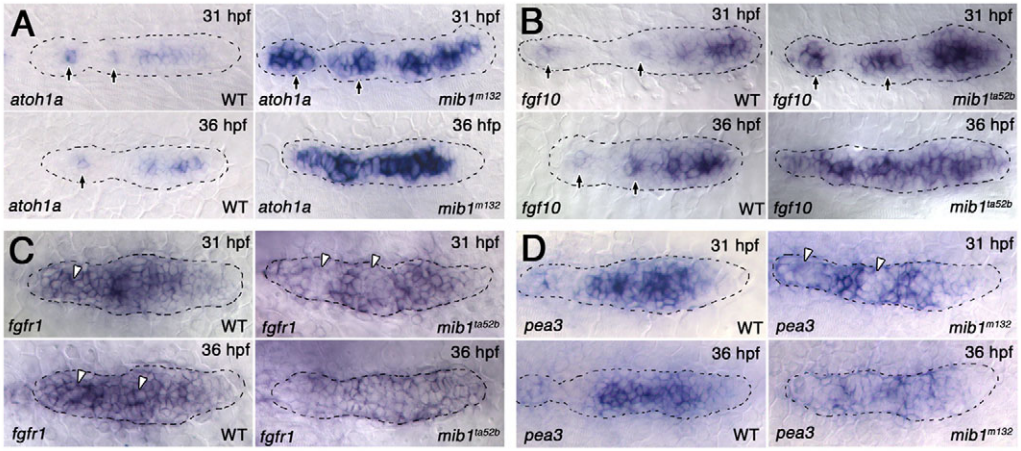


**Fig. 3. Notch signaling regulates expression of FGF signaling components.** (**A**,**B**) *atoh1a* (A) and *fgf10* (B) expression in leading and trailing proneuromasts (arrows) in wild-type and *mib1*$^{ta52b}$ zebrafish embryos at 31 and 36 hpf. There is 1° expansion of *atoh1a* and *fgf10* expression at 31 hpf and 2° expansion by 36 hpf in *mib1*$^{ta52b}$ embryos. (**C**,**D**) *fgfr1* (C) and *pea3* (D) are expressed in a pattern complementary to *atoh1a* and *fgf10* in the pLLp. Although subtle, *fgfr1* and *pea3* expression is reduced in the central cells in maturing proneuromasts (arrowheads). In *mib1*$^{ta52b}$ embryos, *fgfr1* and *pea3* expression is reduced in large clusters of cells (1° reduction) at 31 hpf (arrowheads). *fgfr1* and *pea3* expression is reduced in a broader domain and is restricted to the edges of the pLLp (2° reduction) by 36 hpf.

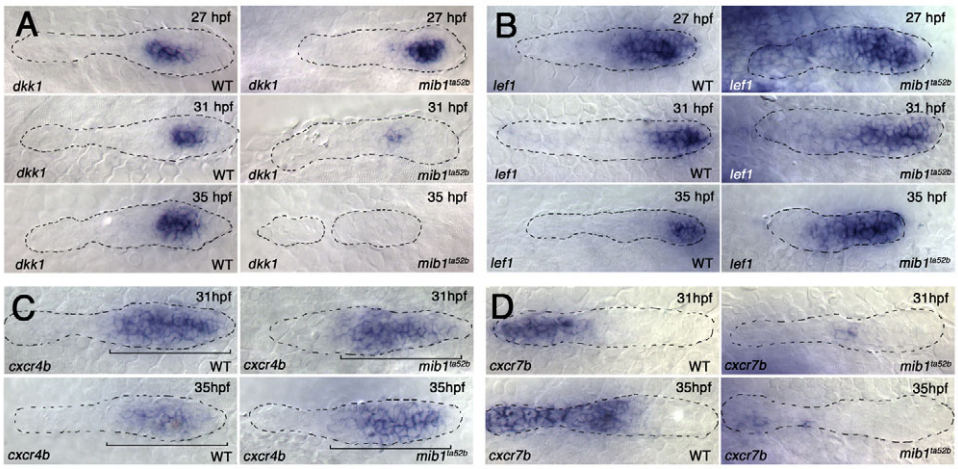


**Fig. 4. Progressive loss of FGF signaling results in loss of FGF-dependent gene expression and in expansion of Wnt-dependent gene expression.** (**A**,**B**) FGF-dependent *dkk1* expression is progressively lost between 27 and 35 hpf in the pLLp of *mib1*$^{ta52b}$ zebrafish embryos (A), whereas the relative size of the *lef1* expression domain progressively expands (B). Note that the *lef1* domain becomes progressively smaller in the older wild-type pLLp. (**C**,**D**) Whereas *cxcr4b* expression (C) is not significantly changed in the *mib1*$^{ta52b}$ pLLp ($n$=7 at 31 hpf and $n$=5 at 35 hpf), *cxcr7b* expression (D) is reduced in *mib1*$^{ta52b}$ by 31 hpf ($n$=9 at 31 hpf and $n$=6 at 35 hpf).

loss of *fgfr1* expression and progressive attenuation of FGF signaling centers, until they are both dramatically weakened and disorganized within the maturing neuromasts. As FGF signaling is required to maintain *fgfr1* expression (Lecaudey et al., 2008; Nechiporuk and Raible, 2008), it is likely that loss of FGF signaling contributes to further loss of *fgfr1* expression within maturing neuromasts.

## Loss of FGF signaling allows expansion of Wnt signaling towards the trailing end

*dkk1* is expressed in an FGF signaling-dependent manner in the youngest proneuromast near the leading end of the pLLp. As a result, failure of FGF signaling was accompanied by a progressive reduction of *dkk1* expression in *mib1*$^{ta52b}$ (Fig. 4A; see Fig. S8A in the supplementary material) and *des*$^{b420}$/N3MO/DAPT (see Fig. S8A and Fig. S9A in the supplementary material) embryos between 27 and 35 hpf. Embryos were classified as having strong, weak or no *dkk1* expression in the pLLp. At 27 hpf, ~30% of the pLLps had no *dkk1* expression, by 31 hpf *dkk1* expression was lost in 45%, and by 35 hpf, which is close to the time when the pLLp typically falls apart, *dkk1* expression was lost in all the embryos examined.

To determine whether loss of the Wnt inhibitor *dkk1* causes expanded Wnt signaling, we examined *lef1* expression, which is dependent on Wnt signaling in the pLLp (Aman and Piotrowski, 2008). The size of the *lef1* domain was significantly larger in *mib1*$^{ta52b}$ mutants than in the wild type at 27, 31 and 35 hpf (Fig. 4B; see Fig. S8B in the supplementary material). Similar expansion of *lef1* expression was seen in *des*$^{b420}$/N3MO/DAPT embryos (see Fig. S9B in the supplementary material).

## The altered balance of FGF and Wnt signaling reduces expression of Cxcr7b in the pLLp

The polarized expression of two chemokine receptors, *cxcr4b* and *cxcr7b*, is essential for effective migration of the pLLp (Dambly-Chaudiere et al., 2007; Haas and Gilmour, 2006; Valentin et al., 2007). As previous studies suggested that Wnt signaling promotes *cxcr4b* expression and suppresses *cxcr7b* expression in the pLLp (Aman and Piotrowski, 2008), we hypothesized that the altered balance of Wnt and FGF signaling would alter their expression and contribute to aberrant migration of the pLLp. In both *mib1*$^{ta52b}$ and *des*$^{b420}$/N3MO/DAPT embryos there was a loss of *cxcr7b* expression (Fig. 4D; see Fig. S7J in the supplementary material), consistent with reduced FGF signaling and/or expanded Wnt activity contributing to reduced *cxcr7b* expression. At the same time, loss of *cxcr7b* expression was not accompanied by a significant change in *cxcr4b* expression (Fig. 4C), suggesting that additional factors prevent expansion of *cxcr4b* expression in the trailing end of the pLLp.

## Knockdown of *atoh1* function can prevent progressive loss of FGF signaling in *mib1* mutants

As unregulated expansion of *atoh1a* following loss of Notch signaling appears to have triggered a chain of events that reduces FGF activity, expands Wnt activation and alters expression of chemokine receptors, we hypothesized that inhibition of *atoh1* function would prevent some of these changes. *atoh1a* and *atoh1b* morpholino (*atoh1*MOs) co-injection in *mib1* mutants successfully prevented unregulated expansion of *fgf10* expression (Fig. 5A) and allowed some recovery of *fgfr1* and *pea3* expression (Fig. 5B; see Fig. S10 in the supplementary material). It also prevented loss of *dkk1* expression (Fig. 5C; see Fig. S11 in the supplementary material) and allowed a partial recovery of *cxcr7b* expression (Fig. 5D).

## Inhibition of *atoh1* function reduces defects in pLLp morphogenesis in *mib1* mutants

We next asked whether reduction of *atoh1* function also prevents any of the problems with pLLp morphogenesis in *mib1* mutants. *atoh1* knockdown appeared to reduce all the defects that develop relatively late during migration in association with progressive expansion of *atoh1a*: it restored formation of the epithelial rosettes within the pLLp (compare Fig. 6B with 6D) and the pLLp migrated further without falling apart (Fig. 6F,H,K,L; see Fig. S3 in the supplementary material). Knockdown of *atoh1* did not, however, restore cohesion of cells in depositing proneuromasts, a defect that develops in *mib1* mutants relatively early during pLLp migration. Instead, it resulted in further loss of cohesion; cells that dissociated from depositing proneuromasts no longer showed a tendency to try and reassociate with previously deposited cells (see Fig. S4C,F and Movie 5 in the supplementary material). Importantly, knockdown of *atoh1* also slightly reduced the size of the depositing neuromasts in wild-type embryos (see Fig. S12 and Movie 6 in the supplementary material). Although it remains unclear why deposited neuromasts are smaller in *atoh1* morphants, one possibility is that *atoh1a* and *mib1* independently contribute to cohesion, such that cohesion in depositing neuromasts is worse in *mib1* mutants when *atoh1a* is knocked down.

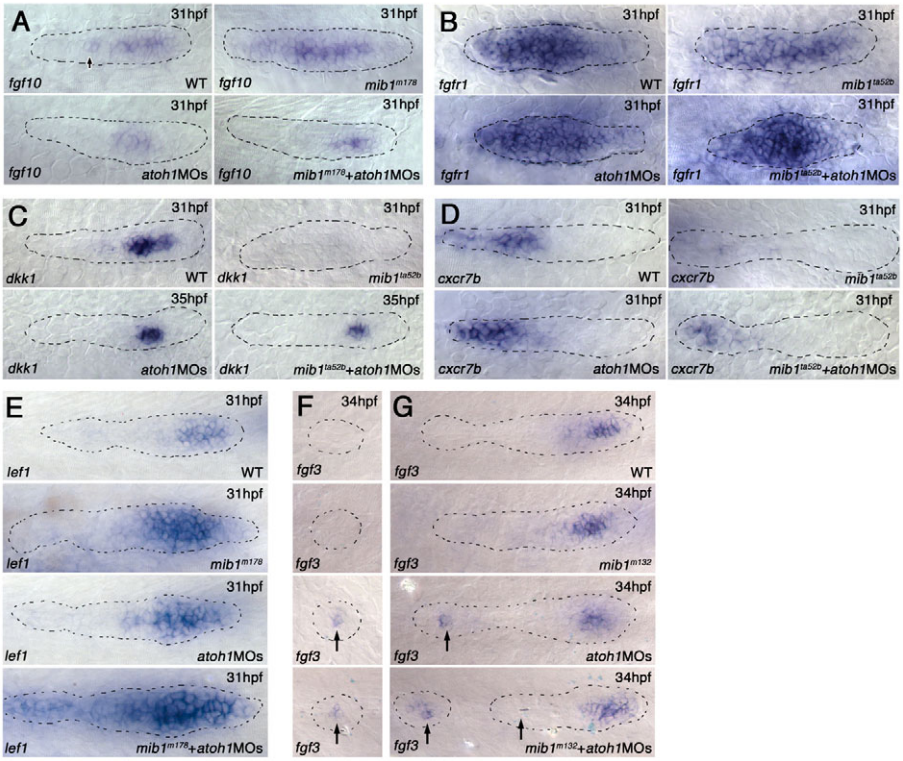


**Fig. 5. Knockdown of *atoh1* function prevents loss of FGF signaling in the *mib1* pLLp.** (**A**,**B**) *atoh1a* and *atoh1b* knockdown prevents unregulated expansion of *fgf10* expression in *mib1* mutant (*mib1*$^{ta52b}$+*atoh1*MOs) zebrafish embryos (*n*=10/10) (A). It also prevents loss of *fgfr1* expression (B). Statistical analysis is shown in Fig. S10A in the supplementary material. (**C**) *dkk1* expression is recovered in *mib1*$^{ta52b}$+*atoh1*MOs embryos. For statistical analysis, see Fig. S11 in the supplementary material. (**D**) *atoh1*MOs allow partial recovery of *cxcr7b* expression in *mib1*$^{ta52b}$ embryos (*n*=5/5). (**E**) *atoh1*MOs allow *lef1* expression to expand further in *mib1*$^{m178}$ mutants. Statistical analysis is shown in Fig. S13 in the supplementary material. (**F**,**G**) Whereas there is no *fgf3* expression in depositing (F) and deposited (G) neuromasts in wild-type (10/10) and *mib1*$^{m132}$ (10/10) embryos, knockdown of *atoh1* results in the persistence of *fgf3* expression in wild-type (7/10) and *mib1*$^{m132}$ (5/10) embryos.

## Knockdown of *atoh1* promotes Wnt-dependent *lef1* expression

Although knockdown of *atoh1* prevented loss of the FGF signaling system and restored FGF-dependent morphogenesis of epithelial rosettes and pLLp migration defects, it did not reduce the size of the *lef1* expression domain in *mib1* mutants. Instead, *lef1* expression became even broader in *atoh1*MOs-injected embryos (Fig. 5E; see Fig. S13 in the supplementary material). This suggests that, although recovery of the pLLp system in *atoh1*MOs-injected *mib1* mutants might have allowed some recovery of FGF signaling, there was no corresponding reduction in the size of the Wnt signaling domain.

As the *atoh1*-dependent FGF signaling system becomes a new source of FGF signals in maturing proneuromasts, it may inhibit persistence of the initial Wnt-dependent FGF signaling system. In *atoh1* morphants, however, a failure to establish the *atoh1*-dependent FGF system might allow the initial Wnt-dependent FGF signaling systems to persist within maturing proneuromasts and account for the expanded *lef1* expression. Consistent with this interpretation, *fgf3*, a component of the original Wnt-FGF system, continued to be expressed in the central cell of depositing and recently deposited neuromasts (Fig. 5F,G) when *atoh1* function was knocked down. It is likely that in the absence of *atoh1*-dependent *fgf10* expression, persistent *fgf3* expression maintains FGF signaling in maturing proneuromasts.

## Changes in pLLp cohesion correlate with changes in Cadherin gene expression

As the pLLp eventually undergoes fragmentation in the absence of Notch signaling, we asked whether this is related to changes in expression of *epithelial cadherin* [*e-cadherin* or *cadherin 1* (*cdh1*)] and *neural cadherin* [*n-cadherin* or *cadherin 2* (*cdh2*)], two cadherins that are expressed in the pLL system (Liu et al., 2003; Kerstetter et al., 2004) and are likely to contribute to cohesive interactions between cells.

In wild-type embryos, *e-cadherin* was at relatively low levels in the leading part of the pLLp, while expression became progressively higher at the trailing end and was relatively intense in depositing neuromasts (Fig. 7A,E). However, *e-cadherin* expression was relatively low in the central *atoh1a*-expressing cell in deposited neuromasts, suggesting that its expression is inhibited in these cells (Fig. 7I,L). Although there was no obvious change in *e-cadherin* expression at 33 hpf (see Fig. S14B in the supplementary material), *e-cadherin* expression was much reduced in the trailing domain of the *mib1*$^{m178}$ pLLp by 37 hpf (Fig. 7B,F). In addition, the central *e-cadherin*-negative domain expanded in deposited neuromasts in *mib1*$^{m178}$ mutants (Fig. 7J,M), suggesting that expanded *atoh1a* expression is eventually associated with reduced *e-cadherin* expression in both the pLLp and deposited neuromasts. Consistent with *atoh1* being associated with inhibition of *e-cadherin* expression, *atoh1*MOs injection expanded *e-cadherin* expression to all the cells within the deposited neuromast in *mib1* mutants (Fig. 7K,N). Whereas *atoh1* knockdown did not significantly alter the overall *e-cadherin* expression pattern in the wild-type pLLp (Fig. 7C,G), it restored higher, wild-type-like expression of *e-cadherin* in the *mib1* pLLp (Fig. 7D,H). The recovery of *e-cadherin* expression was accompanied by improved cell cohesion in the *mib1* pLLp, suggesting that the reduction in *e-cadherin* might contribute to the eventual fragmentation of the pLLp.

In contrast to *e-cadherin*, *n-cadherin* was broadly expressed at the leading end of the pLLp, and its expression became restricted to a central domain in mature proneuromasts as they prepared for deposition (Fig. 7O,Q). It then continued to be expressed in a central cluster of cells in deposited neuromasts (Fig. 7S). Although *n-cadherin* expression overlapped with that of *atoh1a* in the central cell, it was generally broader and included surrounding cells, which were most likely to be prospective support cells that do not express *atoh1a* (Fig. 7T). Although the pattern of *n-cadherin* expression was little changed in *mib1* and *des*$^{b420}$/N3MO/DAPT embryos

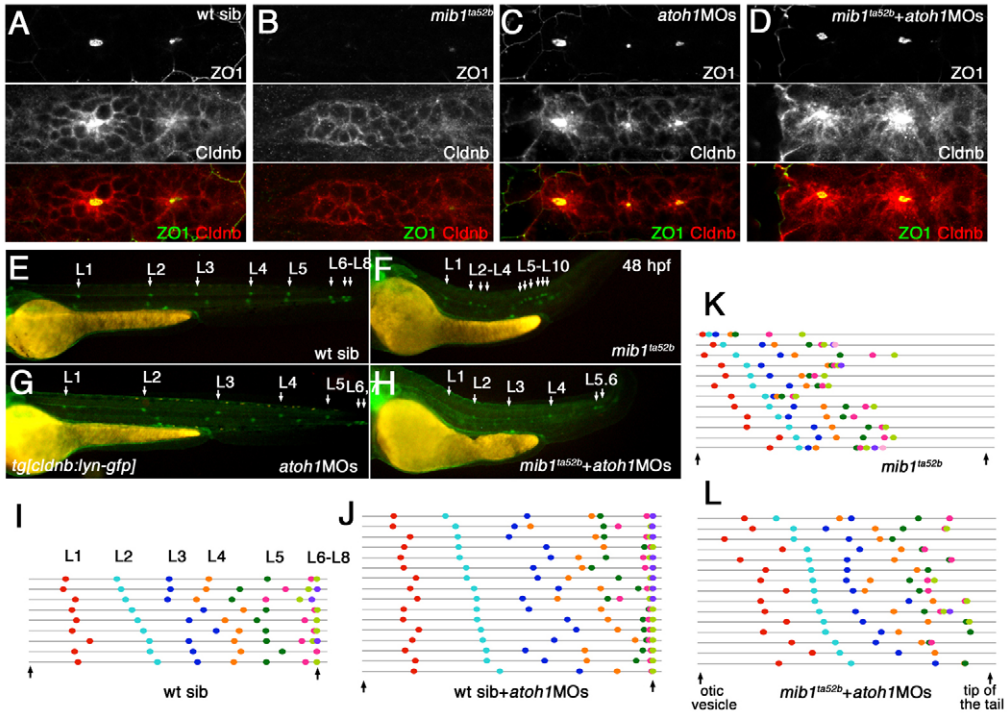


**Fig. 6. Knockdown of *atoh1* reduces some morphogenesis defects in the *mib1* pLLp.** (**A-D**) The central accumulation of ZO1 and Cldnb in maturing proneuromasts (A) is lost in *mib1*$^{ta52b}$ mutants (B), but is recovered when *atoh1* is knocked down (D). (**E-L**) The relative position of deposited neuromasts (L1 to L10) at 48 hpf (E-H). In *mib1*$^{ta52b}$+*atoh1*MOs zebrafish embryos (H), neuromast distribution and pLLp migration are partially rescued. (I-L) Schematic representation of the pattern of neuromast deposition in individual embryos at 48 hpf. For statistical analysis, see Fig. S3 in the supplementary material.

(data not shown), in some embryos there was broader *n-cadherin* expression at the trailing end of the pLLp at 33 hpf (see Fig. S14E in the supplementary material). By 37 hpf, broad expression of *n-cadherin* was seen in isolated groups of cells, which were likely to represent prematurely deposited proneuromasts from a recently fragmented pLLp (Fig. 7P,R; 3/10 embryos). As in wild-type neuromasts, *n-cadherin* continued to be expressed in a central cluster of cells in *mib1*$^{m178}$ mutants, in which it now overlapped with an expanded population of *atoh1a*-expressing hair cell precursors (Fig. 7U,V). Together, these observations suggest that although expanding *atoh1a* expression is eventually associated with progressive suppression of *e-cadherin* expression, it does not dramatically alter *n-cadherin* expression.

Although *atoh1a* knockdown prevented the fragmentation of the pLLp, it did not, as noted before, improve the cohesion of cells in recently deposited or depositing neuromasts in *mib1* mutants (see Fig. S4C,F in the supplementary material). It remains unclear why deposited neuromasts have poor cohesion in *mib1* mutants, but it is not simply related to reduced *e-cadherin*, as expanded *e-cadherin* expression following *atoh1* knockdown does not improve cohesion in deposited neuromasts.

## Distinct regulatory mechanisms regulate Delta and *atoh1a* expression at the leading and trailing ends of the pLLp

DeltaA and DeltaD contribute to the Delta-Notch-mediated lateral inhibition that maintains restricted *atoh1a* expression in maturing proneuromasts. Although their expression patterns are similar, we found that they are differentially regulated by *atoh1a*. Whereas knockdown of *atoh1a* dramatically reduced *deltaD* expression, it had much less effect on *deltaA* (compare Fig. 8A with 8B; see Fig. S1 in the supplementary material for *deltaD* expression in wild-type embryos), suggesting that *atoh1a* does not contribute as much to *deltaA* as to *deltaD* expression. Expression of *deltaA* was, however, progressively eliminated after 1-2 hours of exposure to the FGF signaling inhibitor SU5402 (Fig. 8C), suggesting that FGF signaling is essential for *deltaA* expression. These observations suggest that once *atoh1a* expression is established, it drives expression of *deltaD*, and then both DeltaA and DeltaD ensure that *atoh1a* expression remains restricted to the central cell.

As Atoh1a assumes control of *fgf10* and *deltaD* expression and inhibits *fgfr1* expression in maturing proneuromasts, we asked whether Atoh1a also becomes more responsible for its own expression and less dependent on FGF signaling. When embryos were exposed to SU5402, *atoh1a* expression was lost in the leading domain but retained in the trailing proneuromast following 15 minutes of exposure (Fig. 8D, arrowhead), suggesting that expression in the most mature proneuromast is less dependent on FGF signaling. However, *atoh1a* expression was eventually lost from both the leading and trailing ends of the pLLp by 30 minutes, revealing its continuing dependence on FGF signaling (Fig. 8D).

Mature proneuromasts at the trailing end of the pLLp express *atoh1b*, suggesting that *atoh1b* might help maintain *atoh1a* expression in these proneuromasts. Consistent with this, knockdown of *atoh1b* specifically reduced *atoh1a* expression at the trailing end of the pLLp (Fig. 8E, top). Furthermore, *atoh1a* expression was lost from both the leading and trailing ends of the pLLp within just 15 minutes following exposure to SU5402 when *atoh1b* function was also knocked down (Fig. 8E, bottom; compare with Fig. 8D, middle), showing that normally both FGF signaling and *atoh1b* contribute to maintaining *atoh1a* expression.

Consistent with *atoh1a* determining *atoh1b* expression, expanded *atoh1a* expression in *mib1*$^{ta52b}$ mutants was accompanied by expanded *atoh1b* expression in the trailing proneuromast (compare Fig. 8F with 8G, top), whereas *atoh1b* expression was completely lost in *mib1*$^{ta52b}$ embryos injected with *atoh1a*MO (Fig. 8G, bottom). Interestingly, knockdown of *atoh1a* broadened its own expression at the leading end of the pLLp (Fig. 8H), as loss of *atoh1a*-dependent *deltaD* expression reduced lateral inhibition. However, *atoh1a* expression was not maintained at the trailing end of the pLLp following *atoh1a* knockdown, as self-activation via *atoh1b* is required to maintain high levels of *atoh1a* expression.

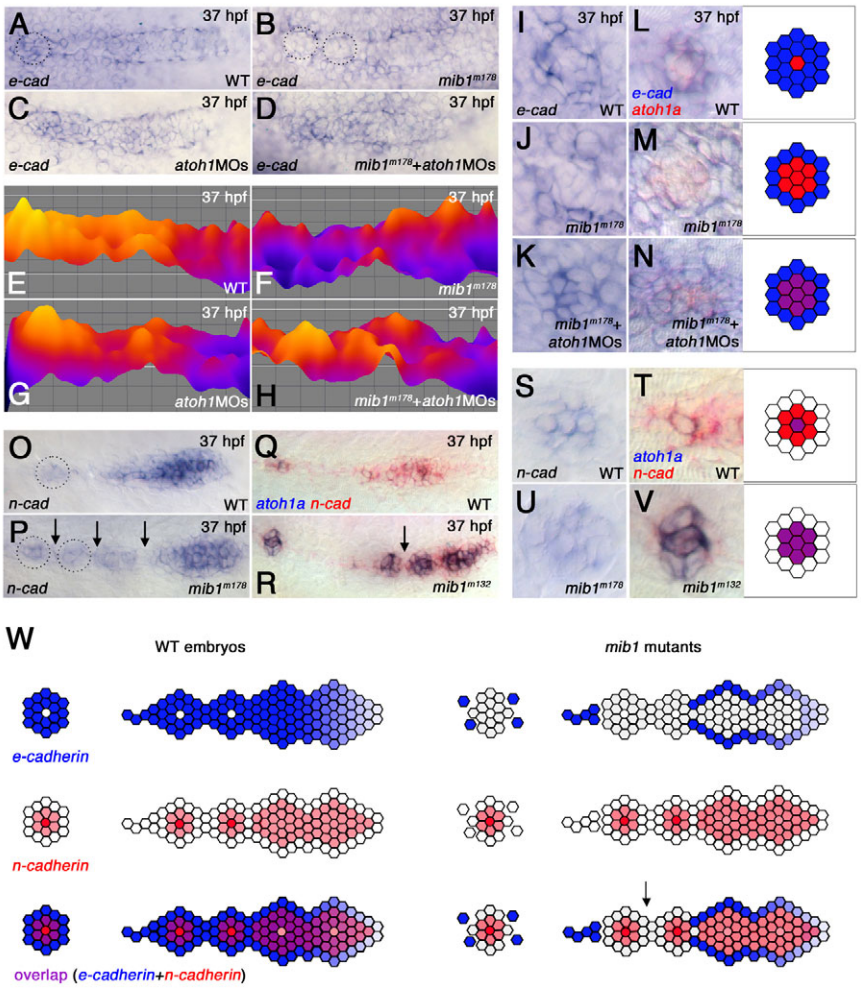


**Fig. 7. Changes in pLLp cohesion correlate with changes in Cadherin gene expression.** (**A-N**) *e-cadherin* expression in the pLLp (A-H) and deposited proneuromasts (I-N) at ~37 hpf. (E-H) Color-coded representations of the *e-cadherin* expression shown in A-D, created using the interactive three-dimensional surface plot plug-in from ImageJ (Abramoff et al., 2004). (A,E) In wild-type, *e-cadherin* is broadly expressed, being lower at the leading and higher at the trailing proneuromasts prior to deposition. (B,F) *e-cadherin* expression is suppressed in the pLLp trailing domain of *mib1*$^{m178}$ zebrafish embryos (*n*=8). Dotted circles in B represent domains of suppressed *e-cadherin* expression. (C,G) *atoh1*MOs do not substantially alter *e-cadherin* expression in wild-type embryos (*n*=7). (D,H) Higher *e-cadherin* expression in the trailing pLLp is restored in *mib1*$^{m178}$+*atoh1*MOs embryos (*n*=12). (I,L) *e-cadherin* expression (blue) is generally more intense, but absent in a central *atoh1a*-expressing cell (red), in deposited neuromasts (*n*=6). (J,M) The central *atoh1a*-expressing domain expands at the cost of *e-cadherin* in *mib1*$^{m178}$ deposited neuromasts (*n*=6). (K,N) Knockdown of *atoh1* in *mib1*$^{m178}$ expands *e-cadherin* expression and allows overlap (purple) with *atoh1a* (*n*=13). (**O-V**) *n-cadherin* expression in the pLLp (O-R) and deposited proneuromasts (S-V). (O,Q) In wild type, *n-cadherin* is broadly expressed at the leading end but becomes restricted at the trailing end, prior to neuromast deposition. (P,R) In *mib1*$^{m178}$ pLLp, *n-cadherin* expression is not significantly different from that of wild type. Dotted circles highlight an example of expanded expression of *n-cadherin* in isolated groups of cells, which are likely to represent prematurely deposited proneuromasts from a recently fragmented pLLp. (Q,R,T,V) Double in situ hybridization showing *atoh1a* (blue) and *n-cadherin* (red) expression. (S-V) In deposited neuromasts, *n-cadherin* expression is similar in wild type (S,T) and *mib1* mutants (U,V). In wild type, a central cell expressing *atoh1a* and *n-cadherin* (purple in T) is surrounded by cells expressing only *n-cadherin* (red in T). In *mib1* mutants, *atoh1a* expands and overlaps with *n-cadherin* (purple in V). (**W**) The pLLp and neuromasts normally contain cells that express *e-cadherin* (blue) or *n-cadherin* (red). Intervening cells expressing both *e-cadherin* and *n-cadherin* (purple) provide an adhesive link between cells that express distinct cadherins. When Notch signaling fails, *atoh1a* expression expands and *e-cadherin* is lost from intervening cells that would otherwise express both Cadherin genes. As *e-cadherin*- and *n-cadherin*-expressing populations are now unable to establish effective adhesive interactions, the pLLp fragments. Arrow indicates predicted point of fragmentation.

## DISCUSSION

In this study we have characterized defects in the morphogenesis of the pLLp system in *mib1* mutants and shown that loss of Notch signaling allows unregulated *atoh1a* expression in the pLLp. This in turn eventually alters FGF, Wnt and chemokine signaling and Cadherin expression, all of which contribute in distinct ways to the aberrant morphogenesis of the pLL system.

Key to understanding how loss of Notch signaling affects pLLp morphogenesis was the discovery that two distinct FGF signaling systems operate in proneuromasts at the leading versus trailing end of the pLLp. Previous studies have shown that a Wnt-dependent FGF signaling system initiates proneuromast formation at the leading end of the pLLp by driving *atoh1a* expression and epithelial rosette formation (Fig. 9A). Our studies suggest that this

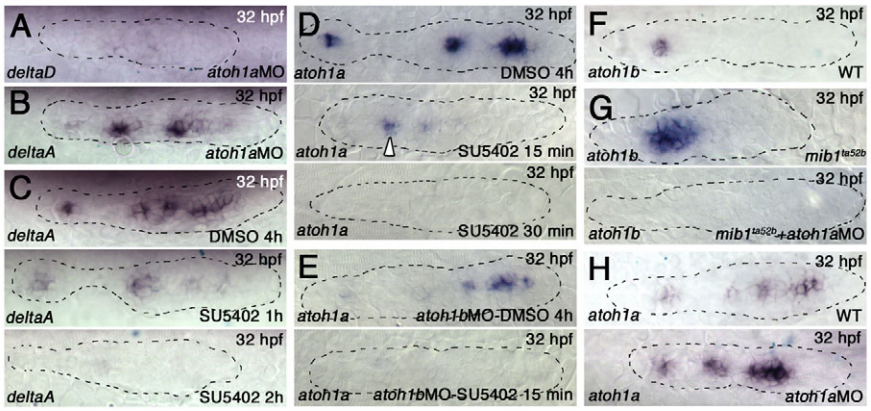


**Fig. 8. *atoh1a* and *atoh1b* cross-activation and establishment of a focal FGF signaling center.** (**A**,**B**) *atoh1*MOs eliminate *deltaD* (A), but not *deltaA* (B), expression in the pLLp of wild-type zebrafish embryos. (**C**) SU5402 treatment eliminates *deltaA* expression after 2 hours. (**D**) *atoh1a* expression is retained in the trailing proneuromasts following 15 minutes of SU5402 exposure (middle), but is lost by 30 minutes (bottom). (**E**) *atoh1b* knockdown reduces *atoh1a* expression in the trailing neuromast (top). *atoh1b* knockdown accompanied by SU5402 exposure for 15 minutes reduces *atoh1a* expression throughout the entire pLLp (bottom). (**F**) *atoh1b* expression is restricted to the trailing neuromast. (**G**) *atoh1b* expression expands in *mib1*$^{ta52b}$ pLLps (top) but is lost when *atoh1a* MO is injected (bottom). (**H**) knockdown of *atoh1a* expands *atoh1a* expression at the leading end, but expanded expression is not maintained at the trailing end (bottom).

FGF signaling system initiates expression of both *atoh1a* and the Notch ligand *deltaA*. In the context of this early expression, DeltaA activates Notch in neighboring cells, inhibits *atoh1a* expression and restricts initial *atoh1a* expression to a central cell. Atoh1a then initiates *deltaD* expression and together DeltaA and DeltaD mediate lateral inhibition to maintain restricted *atoh1a* expression.

Once *atoh1a* expression is stabilized in maturing neuromasts, we suggest that it establishes a second *atoh1a*-dependent FGF signaling system. Atoh1a drives expression of *fgf10* and prevents *fgfr1* expression (Fig. 9A,B, blue cells). Absence of *atoh1a* expression allows the surrounding cells to express *fgfr1* (Fig. 9A,B, yellow cells). Fgf10 expressed by a central cell then activates Fgfr1 in its surrounding cells, ensuring that they maintain expression of Fgfr1 and Notch3, as expression of both is dependent on FGF signaling (data not shown). This ensures that surrounding cells remain competent to receive Delta and FGF signals from the central cell. By contrast, relatively low FGF signaling in the central cell (Fig. 9A,B, blue cells) prevents it from maintaining *fgfr1* and *notch3* expression, which is likely to reduce FGF and Notch pathway activation. As FGF signaling reduces in the central *atoh1a*-expressing cell, *atoh1a* expression becomes progressively less dependent on FGF signaling and more dependent on self-activation: *atoh1a* drives *atoh1b* expression, which in turn drives *atoh1a* expression (Fig. 9A,B, blue cells).

Formation of the *atoh1a*-dependent FGF system in maturing neuromasts establishes a new vulnerability in the pLLp. Maintenance of stability in this system depends on effective Notch-mediated lateral inhibition. When Notch signaling is reduced, *atoh1a* expression can be induced in neighboring cells by FGF signaling (Fig. 9B, black cells). These cells express *fgf10* (Fig. 9B, blue cells) and induce *atoh1a* in their neighbors, eventually resulting in progressive expansion of both *atoh1* and *fgf10* expression. This expansion is accompanied by a complementary loss of *fgfr1* expression (Fig. 9B, yellow cells), a reduction in FGF signaling and a failure to maintain focal FGF signaling centers within maturing proneuromasts. It is important to note that the expansion of *atoh1a* expression and subsequent reduction of FGF signaling is progressive. Eventually, a tipping point is reached, resulting in breakdown of the pLL system. The timing of this event is variable and likely to depend on the severity of loss of Notch signaling. Inhibition of Notch signaling by DAPT alone or reduction of Notch function also results in expansion of *atoh1a* expression and reduction of *fgfr1* expression (data not shown). However, we suspect that fragmentation of the system typically does not take place in this situation because the progressive event takes longer to develop and the pLLp might reach its destination before the 'catastrophe' develops. In principle, it is possible that DAPT contributes to the defects in pLLp morphogenesis by influencing the function of γ-secretase substrates other than Notch, such as Cadherins (Park et al., 2008). However, inhibition of Notch signaling is likely to be the most relevant mechanism, as development of severe morphological defects only accompanies manipulations that also cause loss of Notch-dependent *her4* expression and many of the changes can be linked to the unregulated *atoh1a* expression that results from loss of Notch signaling.

Cells at the leading end actively direct caudal migration of the pLLp, and collective migration of pLLp cells critically depends on the cohesive properties of the cells. We suggest that the loss of *e-cadherin* expression that follows the unregulated expansion of *atoh1a*-expressing cells reduces cohesion and contributes to the eventual fragmentation of the pLLp. This is supported by the observation that knockdown of *atoh1* is accompanied by both a recovery of *e-cadherin* expression and of cohesive integrity of the migrating pLLp. A decrease in *e-cadherin* expression, especially when accompanied by a relative increase of *n-cadherin* expression, has previously been associated with the epithelial-mesenchymal transition that takes place when cancer cells undergo a metastatic transformation (reviewed by Cavallaro and Christofori, 2004). In a similar manner, loss of *e-cadherin* may result in a loss of epithelial integrity and in a failure to maintain the cohesive interactions required for collective migration of the pLLp. Of course, additional adhesion factors similarly affected by *atoh1a* expression might also contribute to pLLp cohesion.

Whereas *e-cadherin* is specifically reduced/excluded from the central *atoh1a*-expressing cell (Fig. 7W, blue cells), *n-cadherin* is normally expressed in a central cell cluster (Fig. 7W, red cells), including both the central *atoh1a*-expressing cell and surrounding prospective support cells that are prevented from expressing

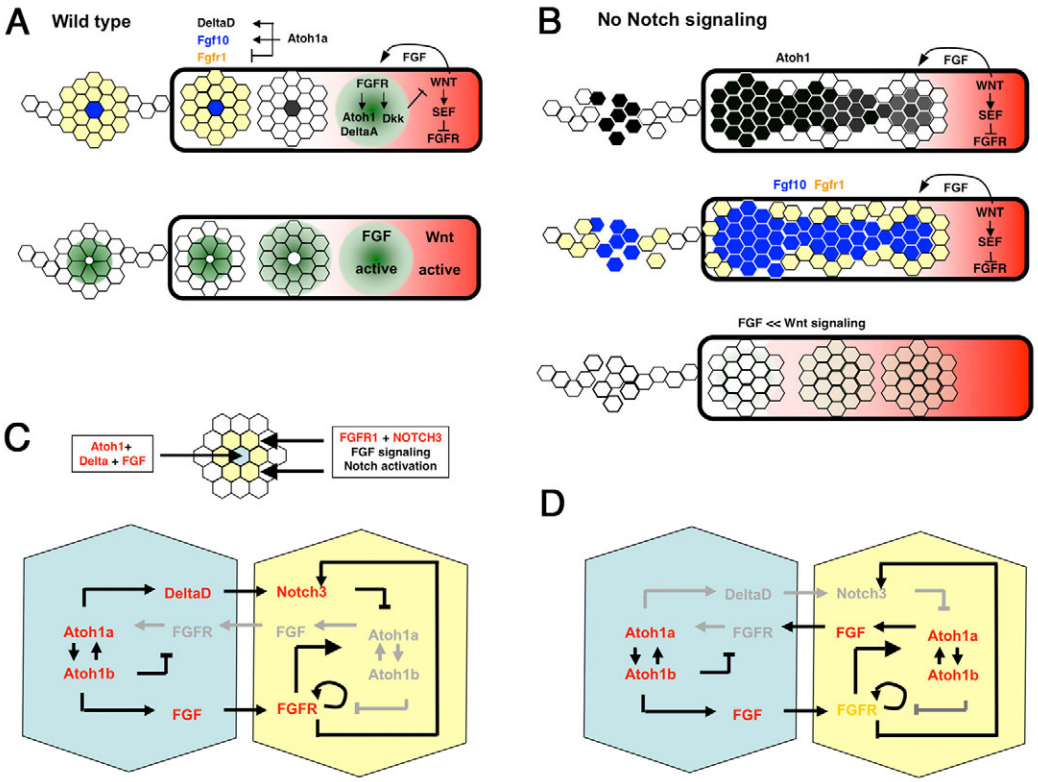


**Fig. 9. Establishment of a focal FGF signaling center by *atoh1* in maturing proneuromasts.** (**A**) Wnt activation (red) drives FGF and *sef* expression, prevents local FGF activation and promotes FGF signaling (green) in an adjacent domain. FGF activation drives expression of the Wnt antagonist *dkk1* and of *atoh1a* and *deltaA*. Delta activates Notch in neighboring cells to restrict *atoh1a* expression to a central cell (black). *atoh1a* drives expression of *fgf10* (blue) and inhibits *fgfr1*(yellow), establishing a focal FGF signaling system. (**B**) In the absence of Notch signaling, additional cells express *atoh1a* and *fgf10*, then shut off *fgfr1*. This results in progressive loss of active FGF signaling, loss of *dkk1*, and expansion of Wnt activation. (**C**) Detail of interactions between the central Atoh-expressing cell (blue) and surrounding cells (yellow). Atoh1a-Atoh1b cross-regulation helps maintain *atoh1* expression in the central cell. Delta and FGF activate Notch and Fgfr1 in surrounding cells. *fgfr1* expression is maintained by autoregulation. FGF activation maintains *notch3* expression. Notch inhibits *atoh1a* expression in surrounding cells. (**D**) In the absence of Notch activation, surrounding cells (yellow) initiate *atoh1a* expression; this initiates FGF expression, suppresses Fgfr1 expression, reduces FGF signaling and eventually leads to loss of Notch3 expression.

*atoh1a*. This implies that support cells express both *e-cadherin* and *n-cadherin* (Fig. 7W, purple cells) and could potentially form effective adhesive junctions with both outer non-sensory cells that express only *e-cadherin* (Fig. 7W, blue cells) and inner sensory hair cell precursors that express only *n-cadherin* (Fig. 7W, red cells). In the absence of Notch signaling, as prospective support cells express *atoh1a* and are mis-specified as hair cell precursors, they would lose *e-cadherin* expression and no longer make effective junctional complexes with surrounding *e-cadherin*-expressing cells (Fig. 7W, no purple cells in maturing proneuromasts). This could ultimately contribute to pLLp fragmentation.

The possibility that support cells provide an essential adhesive link between sensory hair cells and surrounding non-sensory cells first emerged from ultrastructural analysis of the ear in zebrafish *mib1* mutants, in which the sensory hair cell population expands at the cost of surrounding support cells (Haddon et al., 1999). This study showed that the expanded population of hair cells is expelled from the ear epithelium because effective junctional complexes do not form between hair cells and surrounding non-sensory cells in the absence of support cells. It was suggested that two distinct homophilic adhesion proteins might determine cohesive interactions between hair cells and between non-sensory cells. By expressing both of the homophilic adhesion proteins, support cells could form adhesive interactions with both hair cells and the surrounding outer non-sensory cells, and in this manner serve as the adhesive link between these two cell populations. Our analysis of *e-cadherin* and *n-cadherin* expression suggests a very similar role for support cells in the pLLp system and provides preliminary evidence for the predicted pattern of homophilic adhesion factor expression in hair cells, support cells and surrounding non-sensory cells.

Having shown that unregulated expansion of *atoh1a* expression can result in a cascade of defects that contribute to aberrant pLLp morphogenesis in *mib1* mutants, we showed that inhibition of *atoh1a* function prevents many of these problems. This suggests that although *atoh1a* normally assumes significant control of FGF signaling in proneuromasts at the trailing end of the pLLp, the establishment of the *atoh1a*-dependent FGF signaling system is completely dispensable for many aspects of pLLp morphogenesis. What, then, is the significance of the *atoh1a*-dependent FGF signaling center?

Examination of hair cell precursors with DeltaD antibody shows that the specified sensory hair cell is always precisely at the center of the maturing neuromast (see Fig. S15 in the supplementary material). By determining both the sensory hair cell fate and morphogenesis of center-oriented epithelial rosettes, we suggest that the *atoh1*-dependent FGF system provides a robust mechanism to coordinate cell fate and morphogenesis in maturing neuromasts. The remarkable potential of neuromasts for regulated growth and

regeneration emerges from the capacity of the central cells to serve as a source of FGF signals that can induce further *atoh1a* expression in neighbors. The specification of additional *atoh1a*-expressing cells remains, however, under tight regulation by Notch signaling, which determines when and how many *atoh1a*-expressing cells are induced by FGF signaling.

Simultaneous DAPT treatment and Notch gene knockdown does not recapitulate the very early defects in cohesion observed in cells of depositing proneuromasts in *mib1*$^{ta52b}$ mutants (see Fig. S4 in the supplementary material). One interpretation is that these early defects reflect a quantitative difference in the severity of Notch signaling rather than a qualitatively distinct phenomenon. However, additional proteins that are functionally regulated by Mib1 might contribute to defects in cohesion. Additional Mib1-interacting proteins have been identified both by us and other groups (Jin et al., 2002; Choe et al., 2007; Ossipova et al., 2009) (our unpublished data). We are now investigating their function with a view to identifying additional mechanisms by which Mib1 might regulate cell cohesion during epithelial morphogenesis.

It should be noted that although this study focuses on changes within the pLLp that contribute to its aberrant morphogenesis in *mib1* mutants, there are changes along its migratory path that are also likely to contribute. For example, there is an increase in the expression of the chemokine *sdf1a* (cxcl12a – Zebrafish Information Network) along its migratory path (see Fig. S16 in the supplementary material), which is also likely to influence pLLp migration.

In summary, our study has identified a role for Notch-restricted *atoh1a* expression in establishing a focal FGF signaling center in maturing proneuromasts. It emphasizes the importance of understanding the interconnection of different signaling systems within a developing organ. It also illustrates how changes in the regulatory network within the pLLp contribute to the self-organization of neuromasts as they form sensory organs with the potential for growth and regeneration, and how the failure of a key node in the genetic network can have wide-ranging effects on cell fate and cell behavior in the pLLp system.

**Acknowledgements**

We thank James Hudspeth, Rockefeller University, NY, USA, for providing anti-Claudin b antibody, Motoyuki Itoh for preliminary exploration of these questions, and all members of the A.B.C. laboratory for their comments. This work was supported by the Intramural Research Program of the NIH/NICHD. Deposited in PMC for immediate release. This article is freely accessible online from the date of publication.

**Competing interests statement**

The authors declare no competing financial interests.

**Supplementary material**

Supplementary material for this article is available at
http://dev.biologists.org/lookup/suppl/doi:10.1242/dev.052761/-/DC1

**References**

**Abramoff, M. D., Magelhaes, P. J. and Ram, S. J.** (2004). Image processing with ImageJ. *Biophotonics Int.* **11**, 36-42.
**Aman, A. and Piotrowski, T.** (2008). Wnt/beta-catenin and Fgf signaling control collective cell migration by restricting chemokine receptor expression. *Dev. Cell* **15**, 749-761.
**Cavallaro, U. and Christofori, G.** (2004). Cell adhesion and signalling by cadherins and Ig-CAMs in cancer. *Nat. Rev. Cancer* **4**, 118-132.
**Choe, E. A., Liao, L., Zhou, J. Y., Cheng, D., Duong, D. M., Jin, P., Tsai, L. H. and Peng, J.** (2007). Neuronal morphogenesis is regulated by the interplay between cyclin-dependent kinase 5 and the ubiquitin ligase mind bomb 1. *J. Neurosci.* **27**, 9503-9512.
**D'Souza, B., Miyamoto, A. and Weinmaster, G.** (2008). The many facets of Notch ligands. *Oncogene* **27**, 5148-5167.
**Dambly-Chaudiere, C., Cubedo, N. and Ghysen, A.** (2007). Control of cell migration in the development of the posterior lateral line: antagonistic interactions between the chemokine receptors CXCR4 and CXCR7/RDC1. *BMC Dev. Biol.* **7**, 23.
**Geling, A., Steiner, H., Willem, M., Bally-Cuif, L. and Haass, C.** (2002). A gamma-secretase inhibitor blocks Notch signaling in vivo and causes a severe neurogenic phenotype in zebrafish. *EMBO Rep.* **3**, 688-694.
**Ghysen, A. and Dambly-Chaudiere, C.** (2007). The lateral line microcosmos. *Genes Dev.* **21**, 2118-2130.
**Gray, M., Moens, C. B., Amacher, S. L., Eisen, J. S. and Beattie, C. E.** (2001). Zebrafish deadly seven functions in neurogenesis. *Dev. Biol.* **237**, 306-323.
**Haas, P. and Gilmour, D.** (2006). Chemokine signaling mediates self-organizing tissue migration in the zebrafish lateral line. *Dev. Cell* **10**, 673-680.
**Haddon, C., Mowbray, C., Whitfield, T., Jones, D., Gschmeissner, S. and Lewis, J.** (1999). Hair cells without supporting cells: further studies in the ear of the zebrafish mind bomb mutant. *J. Neurocytol.* **28**, 837-850.
**Itoh, M. and Chitnis, A. B.** (2001). Expression of proneural and neurogenic genes in the zebrafish lateral line primordium correlates with selection of hair cell fate in neuromasts. *Mech. Dev.* **102**, 263-266.
**Itoh, M., Kim, C. H., Palardy, G., Oda, T., Jiang, Y. J., Maust, D., Yeo, S. Y., Lorick, K., Wright, G. J., Ariza-McNaughton, L. et al.** (2003). Mind bomb is a ubiquitin ligase that is essential for efficient activation of Notch signaling by Delta. *Dev. Cell* **4**, 67-82.
**Jiang, Y. J., Brand, M., Heisenberg, C. P., Beuchle, D., Furutani-Seiki, M., Kelsh, R. N., Warga, R. M., Granato, M., Haffter, P., Hammerschmidt, M. et al.** (1996). Mutations affecting neurogenesis and brain morphology in the zebrafish, Danio rerio. *Development* **123**, 205-216.
**Jin, Y., Blue, E. K., Dixon, S., Shao, Z. and Gallagher, P. J.** (2002). A death-associated protein kinase (DAPK)-interacting protein, DIP-1, is an E3 ubiquitin ligase that promotes tumor necrosis factor-induced apoptosis and regulates the cellular levels of DAPK. *J. Biol. Chem.* **277**, 46980-46986.
**Jowett, T.** (2001). Double in situ hybridization techniques in zebrafish. *Methods* **23**, 345-358.
**Kamei, M. and Weinstein, B. M.** (2005). Long-term time-lapse fluorescence imaging of developing zebrafish. *Zebrafish* **2**, 113-123.
**Kerstetter, A. E., Azodi, E., Marrs, J. A. and Liu, Q.** (2004). Cadherin-2 function in the cranial ganglia and lateral line system of developing zebrafish. *Dev. Dyn.* **230**, 137-143.
**Kimmel, C. B., Ballard, W. W., Kimmel, S. R., Ullmann, B. and Schilling, T. F.** (1995). Stages of embryonic development of the zebrafish. *Dev. Dyn.* **203**, 253-310.
**Lecaudey, V., Cakan-Akdogan, G., Norton, W. H. and Gilmour, D.** (2008). Dynamic Fgf signaling couples morphogenesis and migration in the zebrafish lateral line primordium. *Development* **135**, 2695-2705.
**Liu, Q., Ensign, R. D. and Azodi, E.** (2003). Cadherin-1, -2 and -4 expression in the cranial ganglia and lateral line system of developing zebrafish. *Gene Expr. Patterns* **3**, 653-658.
**Lopez-Schier, H., Starr, C. J., Kappler, J. A., Kollmar, R. and Hudspeth, A. J.** (2004). Directional cell migration establishes the axes of planar polarity in the posterior lateral-line organ of the zebrafish. *Dev. Cell* **7**, 401-412.
**Ma, E. Y. and Raible, D. W.** (2009). Signaling pathways regulating zebrafish lateral line development. *Curr. Biol.* **19**, R381-R386.
**Ma, E. Y., Rubel, E. W. and Raible, D. W.** (2008). Notch signaling regulates the extent of hair cell regeneration in the zebrafish lateral line. *J. Neurosci.* **28**, 2261-2273.
**Matsuda, M. and Chitnis, A. B.** (2009). Interaction with Notch determines endocytosis of specific Delta ligands in zebrafish neural tissue. *Development* **136**, 197-206.
**Millimaki, B. B., Sweet, E. M., Dhason, M. S. and Riley, B. B.** (2007). Zebrafish atoh1 genes: classic proneural activity in the inner ear and regulation by Fgf and Notch. *Development* **134**, 295-305.
**Nechiporuk, A. and Raible, D. W.** (2008). FGF-dependent mechanosensory organ patterning in zebrafish. *Science* **320**, 1774-1777.
**Ossipova, O., Ezan, J. and Sokol, S. Y.** (2009). PAR-1 phosphorylates Mind bomb to promote vertebrate neurogenesis. *Dev. Cell* **17**, 222-233.
**Park, C. S., Kim, O. S., Yun, S. M., Jo, S. A., Jo, I. and Koh, Y. H.** (2008). Presenillin 1/gamma-secretase is associated with cadmium-induced E-cadherin cleavage and COX-2 gene expression in T47D breast cancer cells. *Toxicol. Sci.* **106**, 413-422.
**Robu, M. E., Larson, J. D., Nasevicius, A., Beiraghi, S., Brenner, C., Farber, S. A. and Ekker, S. C.** (2007). p53 activation by knockdown technologies. *PLoS Genet.* **3**, e78.
**Takke, C., Dornseifer, P., v. Weizsacker, E. and Campos-Ortega, J. A.** (1999). her4, a zebrafish homologue of the Drosophila neurogenic gene E(spl), is a target of NOTCH signalling. *Development* **126**, 1811-1821.
**Valentin, G., Haas, P. and Gilmour, D.** (2007). The chemokine SDF1a coordinates tissue migration through the spatially restricted activation of Cxcr7 and Cxcr4b. *Curr. Biol.* **17**, 1026-1031.
**Yeo, S. Y., Kim, M., Kim, H. S., Huh, T. L. and Chitnis, A. B.** (2007). Fluorescent protein expression driven by her4 regulatory elements reveals the spatiotemporal pattern of Notch signaling in the nervous system of zebrafish embryos. *Dev. Biol.* **301**, 555-567.